European Journal of Radiology Open 7 (2020) 100272

Contents lists available at ScienceDirect

European Journal of Radiology Open

journal homepage: www.elsevier.com/locate/ejro

Deep learning for automatic quantification of lung abnormalities in COVID-19 patients: First experience and correlation with clinical parameters

Victor Mergen [a], Adrian Kobe [a], Christian Blüthgen [a], André Euler [a], Thomas Flohr [b], Thomas Frauenfelder [a], Hatem Alkadhi [a], Matthias Eberhard [a,*]

[a] Institute of Diagnostic and Interventional Radiology, University Hospital Zurich, University of Zurich, Switzerland
[b] Siemens Healthineers, Forchheim, Germany

HIGHLIGHTS

- First experience of a deep learning-based tool for lung infection quantification in CT.
- Rapid automatic quantification of lung abnormalities in COVID-19 patients is feasible.
- Software-derived, quantitative CT data correlate with clinical and laboratory parameters.

ARTICLE INFO

Keywords:
Computed tomography
COVID-19
Deep learning
Lung infection

ABSTRACT

Rationale and objectives: To demonstrate the first experience of a deep learning-based algorithm for automatic quantification of lung parenchymal abnormalities in chest CT of COVID-19 patients and to correlate quantitative results with clinical and laboratory parameters.

Materials and methods: We retrospectively included 60 consecutive patients (mean age, 61 ± 12 years; 18 females) with proven COVID-19 infection undergoing chest CT between March and May 2020. Clinical and laboratory data (within 24 h before/after chest CT) were recorded. Prototype software using a deep learning algorithm was applied for automatic segmentation and quantification of lung opacities. Percentage of opacity (PO, ground-glass and consolidations) and percentage of high opacity (PHO, consolidations), were defined as 100 times the volume of segmented abnormalities divided by the volume of the lung mask.

Results: Automatic CT analysis of the lung was feasible in all patients (n = 60). The median time to accomplish automatic evaluation was 120 s (IQR: 118–128 s). In four cases (7 %), manual corrections were necessary. Patients with need for mechanical ventilation had a significantly higher PO (median 44 %, IQR: 23–58 % versus 13 %, IQR: 10–24 %; p = 0.001) and PHO (median: 11 %, IQR: 6–21 % versus 3%, IQR: 2–7 %, p = 0.002) compared to those without. The PO and PHO moderately correlated with c-reactive protein (r = 0.49−0.60, both p < 0.001) and leucocyte count (r = 0.30−0.40, both p = 0.05). PO had a negative correlation with SO_2 (r=−0.50, p = 0.001).

Conclusion: Preliminary experience indicates the feasibility of a rapid, automatic quantification tool of lung parenchymal abnormalities in COVID-19 patients using deep learning, with results correlating with laboratory and clinical parameters.

1. Introduction

In 2020 a novel, highly infectious coronavirus, SARS-CoV-2, rapidly developed to a worldwide pandemic. The clinical appearance of the infection ranges from mild symptoms to fulminant acute respiratory distress syndrome [1–3]. Due to the rapidly growing flood of patients in need for medical care, health care systems were quickly on the verge of collapse. Recent experience showed that it was difficult to respond

* Corresponding author at: Institute of Diagnostic and Interventional Radiology, University Hospital Zurich, Raemistrasse 100, 8091, Zurich, Switzerland.
E-mail address: matthias.eberhard@usz.ch (M. Eberhard).

https://doi.org/10.1016/j.ejro.2020.100272
Received 14 September 2020; Accepted 23 September 2020
Available online 6 October 2020

efficiently to this extreme demand even in developed Western countries [4].

Recently, efforts have been made to implement deep learning-based concepts into medicine to optimize and streamline workflows [5–7]. During the processing of a deep learning-based system a convolutional neural network is trained on a defined, annotated dataset [8]. Subsequently, the algorithm acquires the ability to perform the questioned analysis by itself. In radiology, automated recognition and segmentation of pathology may speed-up diagnosis, quantifies disease, and could help in decision-making processes [9–11].

So far, a few studies assessed the value of machine learning-based algorithms in chest computed tomography (CT) of patients suffering from corona virus infectious disease 2019 (COVID-19) [8,11,12]. Huang et al. [8] quantitatively evaluated disease burden changes over time in patients with different severity of COVID-19 infection using a deep learning-based software, showing differences in the quantity of lung opacification among groups with different disease severity. Li et al. [11] reported the ability of a neural network to accurately diagnose COVID-19 on chest CT distinguishing it from other infectious diseases. Shi et al. [12] developed a deep-learning based model containing five clinical and radiological features to predict the severity of COVID-19 infection, yielding a significantly higher accuracy than a quantitative assessment of CT images alone [12]. From this preliminary experience it can be assumed that full exploitation of machine learning-based computer aided systems might be beneficial in the setting of overwhelming and rapidly increasing patient loads such as that currently occurring during the COVID-19 pandemic.

The purpose of our study was to demonstrate the first experience of a newly developed, deep learning-based algorithm for the automatic quantification of lung parenchymal abnormalities in chest CT of COVID-19 positive patients and to correlate those results with clinical and laboratory parameters.

2. Materials and methods

2.1. Patient population

This retrospective study was approved by the local Ethics Committee and conducted according to the principles of the Declaration of Helsinki. Consent was obtained from all study subjects. We included all 60 consecutive patients (mean age, 61 ± 12 years; 18 females, 42 males) with proven COVID-19 infection who underwent chest CT between March and May 2020 in our hospital. SARS-CoV-2 was confirmed by reverse transcription polymerase chain reaction (RT-PCR) from nasal-pharyngeal swabs in all patients (n = 60). Detailed patient demographics are shown in Table 1.

Clinical data (cough, dyspnea) were recorded at admission, the highest values of laboratory data (c-reactive protein, CRP, leucocytes, interleukin 6, IL-6), temperature, and peripheral oxygen saturation (SO_2) within 24 h before/after chest CT were noted. Need for oxygen supply and mechanical ventilation during hospitalization was noted.

2.2. CT protocol

Patients underwent either non-enhanced (n = 31, 52 %) or contrast-enhanced (n = 29, 48 %) chest CT on a 128-slice single-source CT scanner (SOMATOM Definition Edge Plus; Siemens Healthineers, Forchheim, Germany). Scan parameters were as follows: reference tube voltage 100 kV with automated tube voltage selection (CARE kV); 100 mAs reference tube current-time product with automated attenuation-based tube current modulation (CARE Dose4D); and gantry rotation time 0.28 s. The following reconstruction parameters were applied: sharp convolution kernel; slice increment, 1.0 mm; and slice thickness, 1.5 mm.

Table 1
Patient demographics.

	Count
Baseline characteristics	
No. of patients	60
Age, years (± SD)	61 ± 12
Female sex (%)	18 (30)
Immunosuppression (%)	6 (10)
Body Mass Index (kg/m^2)	26.3 (25.8–28.0)
At presentation:	
Fever (%)	37 (62)
Cough (%)	37 (62)
At CT (+/− 1 day):	
Oxygen supply (%)	12 (20)
Intubation/mechanical ventilation (%)	26 (43)
Temperature [°C]	38.2 ± 1.02
SaO_2	0.90 ± 0.05
Laboratory findings (+/− 1 day of CT)	
CRP [mg/L]	95 (46–185)
IL-6 [ng/L]	65 (32–127)
Leucocytes [G/L]	7.08 (5.17–10.06)

Abbreviations: IQR, inter-quartile range; LDH, lactate dehydrogenase; SD, standard deviation; °C, degrees Celsius; SaO_2, arterial oxygen saturation; CRP, C-reactive protein; IL-6, Interleukin 6.

2.3. CT image data analysis

Images were analysed with the prototype software "syngo.via Frontier CT Lung Infection" (Siemens Healthineers, Forchheim, Germany). As a first step, the software automatically segments the lung and lung lobes on a 3D chest CT data set. Multi-scale deep reinforcement learning is used to detect relevant anatomical landmarks such as the carina bifurcation. These landmarks are used to identify the lung and generate the lung and lobe segmentation with a Deep Image-to-Image Network (DI2IN). The DI2IN was originally trained on a large cohort of patients with various diseases. To improve the robustness of segmentation in infected lung areas, the algorithm was fine-tuned with a patient cohort with ground glass opacities (GGOs), consolidations, and pleural effusions. As a second step, the software automatically segments COVID-19 related abnormalities. A DenseUNet was trained to transfer a 3D chest CT volume to a binary segmentation mask, with all lung voxels containing GGOs or consolidations marked as positive, the rest as negative. 901 CT scans collected between 2002 and 2020 from different institutions from Canada, Europe and the United States were used for the training of the abnormality segmentation. The datasets included 431 COVID-19 pneumonia, 174 other viral pneumonia, and 296 interstitial lung parenchymal disease.

The segmented lung and lung lobes as well as the segmented abnormalities are visualized in an intuitive way (Fig. 1). GGO and consolidations are summarized as *lung opacities*. As a quantitative output, the software provides both the Percentage of Opacity (PO), defined as 100 times the volume of segmented abnormalities divided by the volume of the lung mask, and the Percentage of High Opacity (PHO), defined as 100 times the volume of high opacity regions (consolidations) divided by the volume of the lung mask. These numbers are available for the entire lung and lobe-wise. High-opacity regions were identified using a threshold of -200 Hounsfield Units.

According to the results of quantification, the algorithm adjudicates a 5-point infection score as described by Bernheim et al. [13] with 0 indicating no involvement; 1, less than 25 % involvement (PO < 25); 2, 25–49 % involvement (25 ≤ PO≤49); 3, 50–74 % involvement (50 ≤ PO≤74); and 4, 75–100 % involvement (75 ≤ PO≤100). Further details of the algorithms used herein can be found elsewhere [14].

All CT image analyses were carried out on a standard dedicated workstation (Intel Xeon W-2125 CPU 4.00 GHz; 32.0 GB RAM) at our institution. All automatic analyses were reviewed by a board-certified radiologist and corrected if necessary. The time from starting the automatic CT analysis to the availability of results were recorded. Feasibility

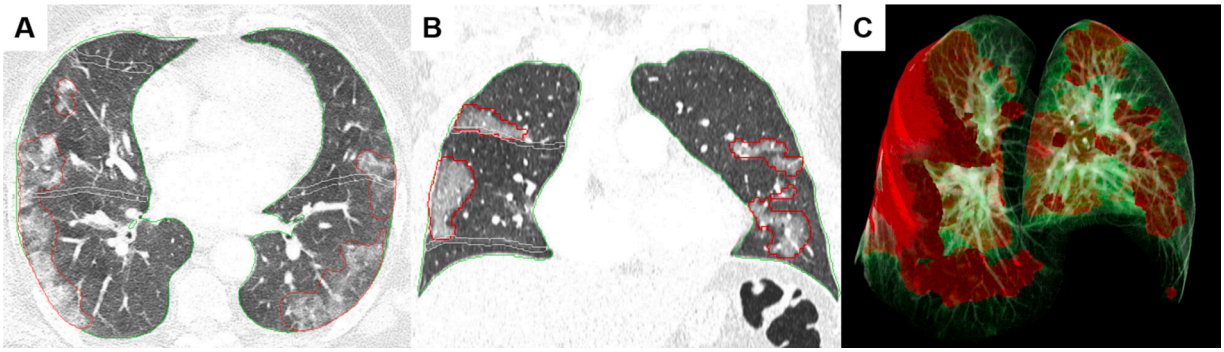

Fig. 1. Example of the result of the automatic segmentation algorithm.
Axial (a) and coronal (b) CT images showing the segmented lung with ground-glass opacities (red line), the entire lung (green line), and the interlobes (white line). 3D reconstruction of the lung (c) visualizes the extent and pattern of abnormal findings in the COVID-19 positive patient.

of automatic CT segmentation was analyzed for each case, and the necessity of manual corrections was assessed.

2.4. Statistical analysis

Normality of continuous data was assessed using the Shapiro-Wilk test. Non-normally distributed continuous data were indicated as median and inter-quartile range (IQR). Normally distributed continuous data were shown as mean ± standard deviation. Sign test, Wilcoxon signed rank test, and the Friedman test were applied to analyze paired data as appropriate. Post-hoc Bonferroni testing was applied for the Friedman test. For correlations, Pearson's correlation or Spearman's rank correlation were applied were appropriate. A two-sided p-value below 0.05 was considered to indicate statistical significance. All analyses were performed with commercially available software (SPSS for Windows 25.0, Chicago, IL, USA).

3. Results

3.1. Patient demographics and CT analysis

Automatic deep learning-based CT analysis of the lung was feasible in all patients (n = 60). The median time to finish the automatic evaluation was 120 s (IQR: 118−128 s). In four cases (7 %) manual corrections were necessary. Two of these cases showed atelectasis which were only partially automatically segmented, and in two cases ground-glass opacities were partially missed by the algorithm.

Fifty-six patients (93 %) had chest CT abnormalities being compatible with COVID-19 pneumonia. 4 patients (7 %) did not have lung opacities.

Median lung volume was 3523 ml (IQR: 2678−4220 ml). Median lung opacity and median lung consolidation were 942 ml (IQR: 354−1427 ml) and 207 ml (66−464 ml), respectively. The median PO and PHO were 28 % (IQR: 11−44 %) and 6 % (IQR: 2–13 %), respectively.

Patients undergoing contrast-enhanced CT showed a higher PHO (median: 10 %, IQR: 4–7 %) compared to patients undergoing non-enhanced CT (4 %, IQR: 2–8 %, p = 0.016). No significant difference was found for the PO between patients undergoing contrast-enhanced CT (35 %, IQR: 22–48 %) and non-enhanced CT (22 %, IQR: 16–48 %, p = 0.056).

The median infection score was 2 (IQR: 1–2), with no significant differences between the right (median: 2, IQR: 1–2) and left lung (median: 2, IQR: 1–2, p = 0.327, Table 2). Furthermore, there were no

Table 2
Results from automatic quantification of lung parenchymal abnormalities using deep learning. Panel A shows details of the segmentation of the entire lung and of the left and right lung separately. Panel B indicates results for each lung lobe.

A		Entire lung	Left lung	Right lung
Affected		56 (93)	53 (88)	56 (93)
	0	4 (7)	7 (12)	4 (7)
	1	25 (42)	22 (37)	22 (37)
Infection Score	2	21 (35)	17 (28)	23 (38)
	3	8 (13)	12 (20)	7 (12)
	4	2 (3)	2 (3)	4 (7)
Lung volume (ml)		3523 (2678−4220)	1580 (1180–1949)	1918 (1481–2332)
Opacity (ml)		942 (354–1427)	337 (128–632)	512 (205–847)
Opacity (%)		28 (11−44)	27 (8–45)	27 (12–44)
Consolidation (ml)		207 (66−464)	78 (18–216)	102 (47–266)
Consolidation (%)		6 (2−12)	5 (1–14)	6 (3–14)
Mean HU total		−627 ± 125	−625 ± 129	−624 ± 132
Mean HU of opacity		−405 ± 124	−410 ± 140	−403 ± 136

B	LUL	LLL	RUL	ML	RLL
Lung volume (ml)	893 (703−1108)	659 (452–907)	752 (610–939)	364 (281–466)	729 (538–978)
Opacity (ml)	151 (14−318)	180 (90–403)	158 (33–324)	36 (7–93)	271 (140–465)
Opacity (%)	17 (2–37) $^{+*}$	46 (11–70)	19 (5–43) *	10 (2–22) $^{+*§}$	44 (21–78)
Consolidation (ml)	17 (3–69)	62 (13–114)	33 (6–56)	5 (1–17)	56 (28–194)
Consolidation (%)	2 (0.3–7) $^{+*}$	9 (2–24)	4 (1–9)	2 (0.4–4) $^{+*§}$	12 (3–30)

Abbreviations: LLL, left lower lobe; LUL, left upper lobe; ML, middle lobe; RLL, right lower lobe; RUL, right upper lobe.
+Significant differences compared to the LLL ($p < 0.05$).
*Significant differences compared to the RLL ($p < 0.05$).
§Significant differences compared to the RUL ($p < 0.05$).

differences in the proportion of PO and PHO between the left and right lung (both, $p > 0.05$).

The left lower lobe (LLL; median: 46 %, IQR: 11–70 %) and the right lower lobe (RLL; median: 44 %, IQR: 21–78 %) showed the highest PO with significant differences compared to the middle lobe (ML) and the left upper lobe (LUL; $p < 0.001$ for all, see Table 2) and between the RLL and the right upper lobe ($p = 0.047$).

The LLL (median: 9 %, IQR: 2–24%) and the RLL (median: 12 %, IQR: 3–30 %) showed the highest PHO with significant differences compared to the ML and the LUL ($p < 0.001$ for all; see Table 2).

3.2. Correlation of quantitative CT with clinical parameters

Patients with need for mechanical ventilation had a significantly higher PO (median 44 %, IQR: 23–58 % versus 13 %, IQR: 10–24 %; $p = 0.001$; Fig. 2a) and PHO (median: 11 %, IQR: 6–21 % versus 3%, IQR: 2–7 %, $p = 0.002$, Fig. 2b) compared to patients without.

PO showed a significant correlation with CRP ($r = 0.60$, $p < 0.001$, Fig. 3a), leucocyte count ($r = 0.40$, $p = 0.002$) and a negative correlation with SO_2 ($r = -0.50$, $p < 0.001$). The PHO showed a moderate correlation with CRP ($r = 0.49$, $p < 0.001$, Fig. 3b) and the leucocyte count ($r = 0.30$, $p = 0.024$).

The infection score significantly correlated with CRP ($r = 0.51$, $p < 0.001$), IL-6 ($r = 0.41$, $p = 0.015$), and leucocyte count ($r = 0.34$, $p = 0.009$), and showed a negative correlation with SO_2 ($r = -0.57$, $p < 0.001$).

4. Discussion

Our preliminary experience indicates the feasibility of an automatic tool for quantification of lung parenchymal abnormalities in COVID-19 patients using deep learning. In our cohort with 93 % patients presenting with characteristic COVID-19 chest CT findings, the algorithm provided rapid results (median time for automatic evaluation 120 s) with only 7% of cases needing manual correction. To our knowledge this is the first study evaluating the correlation between quantitative chest CT findings with laboratory and clinical parameters, showing moderate correlations between PO and PHO with laboratory parameters (CRP, leucocyte count) as well as with SO_2. Patients admitted to the ICU and in need for mechanical ventilation presented significantly higher proportions of PO and PHO compared to those without.

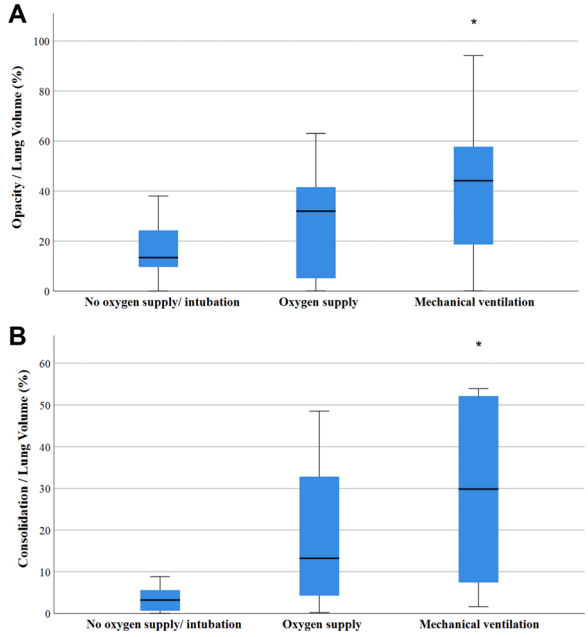

Fig. 2. Proportion of the lung with lung opacity (A) and consolidation (B) in COVID-19 patients stratified according to the need for oxygen supply or mechanical ventilation. Ground-glass opacities and consolidations are summarized as *lung opacities*.
* Significant difference compared to patients without the need for oxygen supply or intubation ($p < 0.05$).

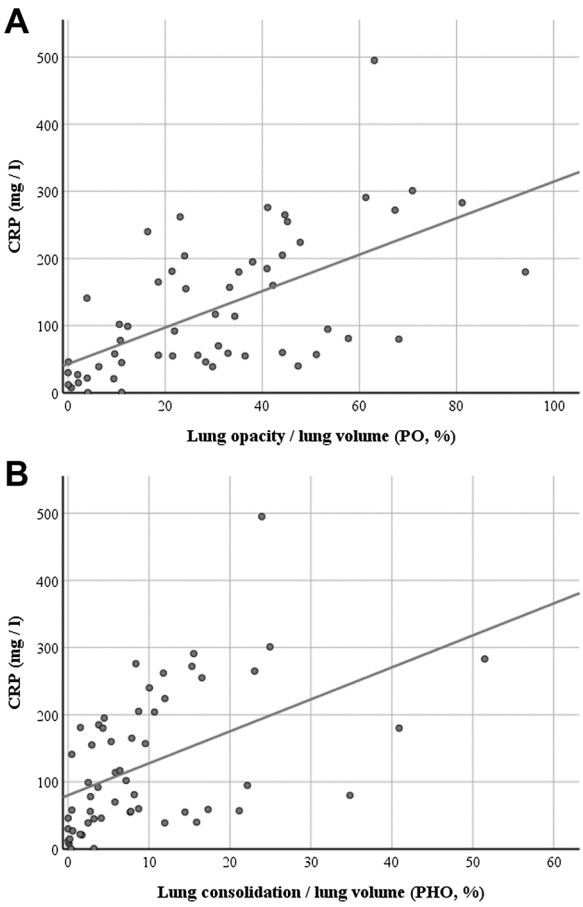

Fig. 3. Correlation of c-reactive protein (CRP) with the proportion of the lung with lung opacity (A) and lung consolidation (B) in COVID-19 patients. Ground-glass opacities and consolidations are summarized as *lung opacities*.

The predominant chest CT findings in early stages of COVID-19 infection are peripheral and subpleural ground glass opacities [2,3,15]. With evolving disease, lung consolidations become the predominant pattern approximately 10 days after onset of symptoms [2,16,17]. Lately, a few reports described initial experiences with automated deep-learning approaches [8,11,12] or semi-automated non-deep learning approaches [18,19] to correctly diagnose COVID-19 or to derive quantitative chest CT results. Huang et al. [8] used a commercially available deep learning algorithm trained on an annotated dataset of COVID-19 patients, providing quantitative results for PO in baseline CT, however, the algorithm did not differentiate between GGO and consolidations. Authors did not manually adjust the automatic segmentation, and 9 % of cases were excluded due to poor segmentation. In 56 out of 212 scans the segmentation indicated a perfect fit with lung opacities, while in the other cases minor imperfections were noted [8].

Shi et al. [12] used a convolutional neural network to quantify the volume of lung infection as well as the percentage of lung infection in COVID-19 positive patients. After training the software with an annotated set of images, the model learned to automatically detect the lung, opacities, and consolidations in chest CT. Differentiation between ground-glass opacities (-750 to -300 HU) and consolidations (−300 to 50 HU) was based on lung attenuation. Neither Shi et al. nor Huang et al. reported the time needed for automatic evaluation [8,12]. Li et al. [11]

reported an average processing time of 5 s for their deep learning algorithm, however, this algorithm was used for disease detection and did not provide quantitative results.

Another approach was applied by Colombi et al. [18] and Lanza et al. [19] determining the value of quantifying the extent of well-aerated lung at baseline chest CT in COVID-19 patients. Both groups used an open-source (not deep learning-based) 3D slicer software to quantify the percentage and absolute volume of well aerated lung in SARS-CoV-2 positive patients at baseline CT. The software used density references to identify normal lung parenchyma. Segmentation was accomplished after a median time of 270 s, and manual correction was necessary in 61 % of cases. Authors observed that software-determined well aerated lung parenchyma of less than 71 % was associated with ICU admission or death.

In our study, a prototype deep-learning based software was applied. Comparing our results to that from Colombi et al. [18], the deep learning algorithm provided a faster (120 s vs. 270 s) and more accurate segmentation with post-hoc corrections only necessary in 7% of cases (vs. 61 %). Lanza et al. [19] reported a median time for segmentation of 11 min. The automatic chest CT analysis in our study was carried out on a standard PACS workstation of our institution. Using faster hardware equipment may speed-up automatic lung evaluation to a significant degree [14].

Similar to previous studies, our study showed that the extent of lung opacities and consolidations increase with laboratory and clinical severity of disease [1,8,12,20], adding objective, quantitative aspects to the analysis of chest CT. Especially in follow-up chest CT, reliable and rapid automatic quantification of abnormalities may support radiologists in determining disease progression or regression. However, we must admit that the number of cases in our study was overall too small, and only a minority of these patients obtained follow-up CT. Thus, evaluating the usefulness of this tool for follow-up CT examinations was not possible.

The following limitations of our study merit consideration. First, the study suffers from inherent shortcomings of a retrospective, single-center approach. Second, CT was acquired during various clinical stages of disease, potentially including bias into the analysis of the correlation between quantitative CT parameters and clinical and laboratory findings. Third, we did not assess whether the deep learning algorithm is able to differentiate patterns of different pulmonary infection. Fourth, we did no compare the accuracy of segmentation of lung parenchymal abnormalities of this algorithm with other automatic tools. Finally, our study lacks mid- and long-term follow-up outcome data to determine the value of such algorithms for patient care.

In conclusion, our preliminary experience indicates the feasibility of a rapid, automatic quantification tool for lung parenchymal abnormalities in COVID-19 patients using deep learning. The algorithm has the potential to speed up chest CT evaluation of COVID-19 positive patients providing quantitative parameters. Future studies should assess whether such parameters may add prognostic value beyond laboratory and clinical results alone.

Source of funding

This research did not receive any specific grant from funding agencies in the public, commercial, or not-for-profit sectors.

Ethics statement

This retrospective study was approved by the local Ethics Committee and conducted according to the principles of the Declaration of Helsinki. Consent was obtained from all study subjects.

Declaration of Competing Interest

Dr. Thomas Flohr is an employee of Siemens Healthineers. The remaining authors declare that the research was conducted in the absence of any commercial or financial relationships that could be construed as a potential conflict of interest.

References

[1] C. Huang, Y. Wang, X. Li, L. Ren, J. Zhao, Y. Hu, L. Zhang, G. Fan, J. Xu, X. Gu, Clinical features of patients infected with 2019 novel coronavirus in Wuhan, China, Lancet 395 (10223) (2020) 497–506.
[2] Y. Xiong, D. Sun, Y. Liu, Y. Fan, L. Zhao, X. Li, W. Zhu, Clinical and high-resolution CT features of the COVID-19 infection: comparison of the initial and follow-up changes, Invest. Radiol. 55 (6) (2020) 332–339.
[3] J. Wu, X. Wu, W. Zeng, D. Guo, Z. Fang, L. Chen, H. Huang, C. Li, Chest CT findings in patients with Coronavirus disease 2019 and its relationship with clinical features, Invest. Radiol. 55 (5) (2020) 257–261.
[4] H.W. Zhang, J. Yu, H.J. Xu, Y. Lei, Z.H. Pu, W.C. Dai, F. Lin, Y.L. Wang, X.L. Wu, L. H. Liu, M. Li, Y.Q. Mo, H. Zhang, S.P. Luo, H. Chen, G.W. Lyu, Z.G. Zhou, W.M. Liu, X.L. Liu, H.Y. Song, F.Z. Chen, L. Zeng, H. Zhong, T.T. Guo, Y.Q. Hu, X.X. Yang, P. N. Liu, D.F. Li, Corona virus international public health emergencies: implications for radiology management, Acad. Radiol. 27 (4) (2020) 463–467.
[5] M. Eberhard, H. Alkadhi, Machine learning and deep neural networks: applications in patient and scan preparation, contrast medium, and radiation dose optimization, J. Thorac. Imaging 35 (2020) S17–S20.
[6] G. Choy, O. Khalilzadeh, M. Michalski, S. Do, A.E. Samir, O.S. Pianykh, J.R. Geis, P. V. Pandharipande, J.A. Brink, K.J. Dreyer, Current applications and future impact of machine learning in radiology, Radiology 288 (2) (2018) 318–328.
[7] S. Kulkarni, N. Seneviratne, M.S. Baig, A.H.A. Khan, Artificial intelligence in medicine: where are we now? Acad. Radiol. 27 (1) (2020) 62–70.
[8] L. Huang, R. Han, T. Ai, P. Yu, H. Kang, Q. Tao, L. Xia, Serial quantitative chest CT assessment of covid-19: deep-learning approach, Radiol. Cardiothoracic Imaging 2 (2) (2020), e200075.
[9] L.M. Pehrson, M.B. Nielsen, C. Ammitzbøl Lauridsen, Automatic pulmonary nodule detection applying deep learning or machine learning algorithms to the LIDC-IDRI database: a systematic review, Diagnostics 9 (1) (2019) 29.
[10] S.M. Lee, J.B. Seo, J. Yun, Y.-H. Cho, J. Vogel-Claussen, M.L. Schiebler, W. B. Gefter, E.J. Van Beek, J.M. Goo, K.S. Lee, Deep learning applications in chest radiography and computed tomography, J. Thorac. Imaging 34 (2) (2019) 75–85.
[11] L. Li, L. Qin, Z. Xu, Y. Yin, X. Wang, B. Kong, J. Bai, Y. Lu, Z. Fang, Q. Song, K. Cao, D. Liu, G. Wang, Q. Xu, X. Fang, S. Zhang, J. Xia, J. Xia, Artificial intelligence distinguishes COVID-19 from community acquired pneumonia on chest CT, Radiology (2020), 200905.
[12] W. Shi, X. Peng, T. Liu, Z. Cheng, H. Lu, S. Yang, J. Zhang, F. Li, M. Wang, X. Zhang, Deep Learning-based Quantitative Computed Tomography Model in Predicting the Severity of COVID-19: a Retrospective Study in 196 Patients, 2020.
[13] A. Bernheim, X. Mei, M. Huang, Y. Yang, Z.A. Fayad, N. Zhang, K. Diao, B. Lin, X. Zhu, K. Li, S. Li, H. Shan, A. Jacobi, M. Chung, Chest CT findings in Coronavirus disease-19 (COVID-19): relationship to duration of infection, Radiology 295 (3) (2020), 200463.
[14] S. Chaganti, A. Balachandran, G. Chabin, S. Cohen, T. Flohr, B. Georgescu, P. Grenier, S. Grbic, S. Liu, F. Mellot, N. Murray, S. Nicolaou, W. Parker, T. Re, P. Sanelli, A.W. Sauter, Z. Xu, Y. Yoo, V. Ziebandt, D. Comaniciu, Quantification of Tomographic Patterns Associated with COVID-19 from Chest CT, ArXiv, 2020.
[15] C.S. Guan, Z.B. Lv, S. Yan, Y.N. Du, H. Chen, L.G. Wei, R.M. Xie, B.D. Chen, Imaging features of Coronavirus disease 2019 (COVID-19): evaluation on thin-section CT, Acad. Radiol. 27 (5) (2020) 609–613.
[16] P. Lomoro, F. Verde, F. Zerboni, I. Simonetti, C. Borghi, C. Fachinetti, A. Natalizi, A. Martegani, COVID-19 pneumonia manifestations at the admission on chest ultrasound, radiographs, and CT: single-center study and comprehensive radiologic literature review, Eur. J. Radiol. Open 7 (2020), 100231.
[17] M. El Homsi, M. Chung, A. Bernheim, A. Jacobi, M.J. King, S. Lewis, B. Taouli, Review of chest CT manifestations of COVID-19 infection, Eur. J. Radiol. Open 7 (2020), 100239.
[18] D. Colombi, F.C. Bodini, M. Petrini, G. Maffi, N. Morelli, G. Milanese, M. Silva, N. Sverzellati, E. Michieletti, Well-aerated lung on admitting chest CT to predict adverse outcome in COVID-19 pneumonia, Radiology (2020), 201433.
[19] E. Lanza, R. Muglia, I. Bolengo, O.G. Santonocito, C. Lisi, G. Angelotti, P. Morandini, V. Savevski, L.S. Politi, L. Balzarini, Quantitative chest CT analysis in COVID-19 to predict the need for oxygenation support and intubation, Eur. Radiol. (2020) 1–9, https://doi.org/10.1007/s00330-020-07013-2.
[20] H. Shi, X. Han, N. Jiang, Y. Cao, O. Alwalid, J. Gu, Y. Fan, C. Zheng, Radiological findings from 81 patients with COVID-19 pneumonia in Wuhan, China: a descriptive study, Lancet Infect. Dis. 20 (4) (2020) 425–434, https://doi.org/10.1016/S1473-3099(20)30086-4.